
Article:
Beevers, J. E., Love, C. J., Lazarov, V. K. orcid.org/0000-0002-4314-6865 et al. (6 more authors) (2018) Enhanced magnetoelectric effect in M-type hexaferrites by Co substitution into trigonal bi-pyramidal sites. Applied Physics Letters. 082401. pp. 1-6. ISSN: 0003-6951

https://doi.org/10.1063/1.5017683

Enhanced MagnetoElectric Effect in M-type Hexaferrites by Co substitution into Trigonal Bi-pyramidal Sites

J.E. Beevers[1], C. J. Love[1,3], V. Lazarov[1] and S. A. Cavill[1,3*]
H. Izadkhah[2] and C. Vittoria[2]
R. Fan[3], G. van der Laan[3] and S. S. Dhesi[3]

[1] Department of Physics, The University of York, Heslington, York, YO10 5DD, UK
[2] Department of Electrical and Computer Engineering, Northeastern University, Boston, Massachusetts 02115, USA
[3] Diamond Light Source, Harwell Science and Innovation Campus, Didcot, Oxon OX11 0DE, UK

*email: stuart.cavill@york.ac.uk

Abstract

The magnetoelectric effect in M-type Ti-Co doped strontium hexaferrite has been studied using a combination of magnetometry and element specific soft X-ray spectroscopies. A large increase (> x30) in the magnetoelectric coefficient is found when Co^{2+} enters the trigonal bi-pyramidal site. The 5-fold trigonal bi-pyramidal site has been shown to provide an unusual mechanism for electric polarization based on the displacement of magnetic transition metal (TM) ions. For Co entering this site, an off-centre displacement of the cation may induce a large local electric dipole as well as providing an increased magnetostriction enhancing the magnetoelectric effect.

1. INTRODUCTION

The control of magnetism using applied electric fields offer the possibility of a new generation of ultra-low power, high density storage. In this respect, magnetoelectric (ME) multiferroic materials are intensely studied in order to understand how different symmetry breaking orders exist in the same material and how these orders can be coupled. Among the few room temperature single-phase ME multiferroics reported, hexaferrites show potential for device applications as they exhibit a low field ME effect at room temperature [1].

M-type hexaferrites are arranged in different repeating sequences of basic building blocks; the R and S layers [2]. Fe^{3+} cations occupy both octahedral (O_h) and tetrahedral (T_d) co-ordinated sites in the S block (Wyckoff positions 2a and $4f_1$) and octahedral sites (12k and $4f_2$) in the R block, see online supplementary materials. The Ba ion located at positions 2d strongly distorts the octahedral site located at the 2b positions giving rise to a bi-pyramidal 5 fold co-ordination which induces a large uniaxial magnetic anisotropy parallel to the c-axis [3]. However, Co^{2+} and Ti^{4+} substitutions for Fe^{3+} dramatically alters the magnetic properties [4]. Ti substitutions at the 12k sites decrease the exchange coupling between spins in the R and S blocks whilst Co substitutions change the magnetic anisotropy from uniaxial to an easy cone of magnetization tilted away from the c-axis. The result is to stabilize a non-collinear conical magnetic structure [2,5] which is of high interest in the field of multiferroics [6]. The ME effect at room temperature in $SrFe_8Ti_2Co_2O_{19}$ was first reported in bulk [7] and, thereafter, in thin films [8]. Co^{2+} substitutions in ferrite structures are a well-known source of magnetoelastic coupling due to the large orbital moment of Co^{2+} [9]. The linear ME coupling, α, which is the change in magnetization with an applied electric field is directly proportional to the magnetoelastic coupling, or magnetostriction, λ, implying that an increase in λ increases α [10]. However, a mechanism such as the piezoelectric effect or electrostriction for coupling the applied electric field into strain is also required. Several mechanisms for magnetically induced ferroelectricity have been proposed in recent years [11] with the spin current (or inverse Dzyaloshinskii-Moriya) mechanism in dominant in the

hexaferrites. More recently a unique magnetic-ion induced displacive electric polarization was reported in (Ba,Sr)$Fe_{12}O_{19}$ [12].
In this letter we demonstrate that the magnetoelectric coefficient, α, can be affected in a fundamental way by doping changing the level of Co^{2+} in the 5-fold bi-pyramidal trigonal site.

2. EXPERIMENTAL DETAILS

The samples were grown by pulsed laser deposition (PLD) on 0.3mm thick single crystal sapphire (0001) substrates at 600°C under a 200±5 mtorr partial pressure of oxygen. The alternating target laser deposition technique (ATLAD) was used to deposit Co and Ti ions in the S or R block of the ME hexaferrite material, allowing for different site occupancies compared to deposition from a single target [13]. The R block was grown by depositing from a target of $SrFe_{(4-\delta)}Ti_{0.5\delta}Co_{0.5\delta}O_7$ and the S block by depositing from a target of $Fe_{(1+0.25\delta)}Ti_{0.5(1-0.25\delta)}Co_{0.5(1-0.25\delta)}O_3$. Three samples were grown with δ = 0.0, 0.2 and 0.4 while the chemical formula and crystal structure was held constant, $SrFe_8Ti_2Co_2O_{19}$ as verified by EDX chemical analysis. δ can be considered as a measure of which block the Co-Ti ions reside in. Higher δ values correspond to preferential substitution in the R block. Deposited films were post-annealed in oxygen at 1050 °C for 40 minutes in order to increase the resistivity of the sample [1], and then capped with 2nm of Au. Films thickness's were measured to be 10, 1 and 1 μm for δ = 0.0, 0.2 and 0.4 respectively.
X-ray diffraction (XRD) measurements were performed with a Cu K-alpha source whilst magnetic measurements were performed using a Vibrating Sample Magnetometer (VSM-SQUID). For the ME coupling measurements a voltage, V, was applied across the film and substrate with changes to the magnetization, measured 50 times each 1 second apart by VSM, recorded as a function of V. The reported change is an average of the last 40 measurements after it reaches "steady state". Ti $L_{2,3}$ x-ray absorption spectroscopy (XAS), Co $L_{2,3}$ and Fe $L_{2,3}$ XAS and x-ray magnetic circular dichroism (XMCD) measurements were performed on beamline I06 at the Diamond Light Source [14]. Total-electron yield (TEY) was monitored using the sample drain current.

3. RESULTS

XRD patterns for the two films reveal the hexagonal P63/mmc structure with lattice spacing's of a = 5.87(2) Å, c = 23.05(4) Å for δ = 0, a = 5.84(2) Å, c = 23.05(4) Å for δ = 0.2 and a = 5.87(3) Å, c = 22.93(4) Å for δ = 0.4 which are in good agreement to the range of values found in the literature [2].
VSM magnetometry measurements were performed with the applied field parallel to the surface at 300K, M(H) loops can be found in supplementary materials. At 300K the coercivity for δ = 0, 0.2 and 0.4 are 720, 57 and 32 Oe respectively. The large reduction in coercivity is often attributed to the formation of a cone of magnetization as a result of non-collinearity of the spins in this material [2]. However, it is premature at this point to give a definitive mechanism for the reduction in coercivity.
The magnetoelectric effect is shown in Fig.1 as the change in magnetisation, ΔM, as a function of applied voltage for (a) δ = 0, (b) δ = 0.2 and (c) δ = 0.4. After pre-magnetizing to 20kOe a magnetic field of 400 Oe was applied to ensure a non-zero magnetization from multi-domain formation in which changes due to the application of the electric field could be measured. The measurements were taken with H applied parallel to the applied voltage at 300K.

The magneto-electric coefficient,α, is defined as [15]

$$\alpha = \mu_0 \frac{\partial M}{\partial E}$$

Eq. (1)

where $E = \frac{V}{d}\left(\frac{\varepsilon_s}{\varepsilon_f}\right)$ is the electric field across the film, V is the applied voltage across film and substrate, d is the thickness of the substrate and ε_s, ε_f are the relative permittivities of the substrate and film respectively. The relative permittivity ε_s = 10 for sapphire whilst for M-type hexaferrites ε_f can range from ≈ 20 - 5000 [16, 17] but is highly dependent on the conductivity of the film and therefore the amount of Fe^{2+} in the sample. As the exact d.c value of ε_f for the films are not known, but assumed approximately equal for all three samples due to similar amounts of Fe^{2+}, the ratio of the magnetoelectric coefficients for the films are calculated to give

$$\Lambda_1 = \frac{\alpha(0.2)}{\alpha(0.0)} = 36$$

$$\Lambda_2(1) = \frac{\alpha_1(0.4)}{\alpha(0.0)} = 53 \ , \Lambda_2(2) = \frac{\alpha_2(0.4)}{\alpha(0.0)} = 34$$

For δ = 0.2, α has increased by over an order of magnitude compared to δ = 0.0. For δ = 0.4, there are two linear regions where the gradient and therefore strength of the ME coupling changes with voltage. We therefore give ratios, $\Lambda_2(1)$ and $\Lambda_2(2)$, for these two regions. In agreement with other reports on the M-type hexaferrites [7], the magnetization (M) is reduced on the application of the applied voltage. We note that extrinsic effects, such as current induced phenomena including Joule heating, cannot account for the variation in slopes observed in Fig. 1.

To gain a more detailed understanding of the role of Co-Ti substitutions in SrM, we performed XAS at the Ti $L_{2,3}$ absorption edge and XAS/XMCD measurements at the Co and Fe $L_{2,3}$ absorption edges in order to determine valency, co-ordination and the magnetic response of the individual elements.
Figure 2 shows the Ti XAS measured at the $L_{2,3}$ edges for δ = 0.2. The spectra for δ = 0.0 and 0.4 are nearly identical so only one is plotted. Four peaks are seen in the spectra. In octahedral symmetry, the crystal field splits the degenerate 3d orbitals into an e_g and a t_{2g} configuration. Thus two peaks are expected for each spin orbit split initial state and we find excellent agreement between the experimental data and atomic multiplet calculations [18].
Figure 3 shows XAS and XMCD data for (a,d) δ = 0, (b,e) δ = 0.2 and (c,f) δ = 0.2 at the Fe and Co $L_{2,3}$ edges respectively. Three peaks are present in the XMCD spectra, similar to that found for Fe_3O_4 [19]. These peaks correspond to contributions from Fe^{3+} in octahedral, Fe^{3+} in tetrahedral and Fe^{2+} in octahedral sites. For the M-type hexaferrite structure, spins located at the Fe tetrahedral sites are aligned anti-parallel to the majority of spins at the Fe octahedral sites [2]. Hence the positive peak in the XMCD is due to tetrahedrally co-ordinated Fe^{3+}. Fits to the XMCD data using atomic multiplet calculations show that XMCD spectra is best represented by ~70% octahedral co-ordinated and ~30% tetrahedral co-ordinated Fe. We note that this should not be taken as the relative Fe occupancy of the sites as the spins at the $4f_2$ sites are aligned anti-parallel to the other octahedral sites in the unit cell reducing the octahedral contribution to the XMCD. The occurrence of Fe^{2+} is often found in these materials, probably due to incomplete oxidation during growth. The XAS / XMCD data at the Co $L_{2,3}$ edges is shown in Fig.3(d). The XAS lineshape is a superposition of Co^{2+} spectra in octahedral and

tetrahedral environments. However the XMCD lineshape, which provides information on the uncompensated moments in the ferrimagnetic structure, is predominantly from Co^{2+} in an octahedral environment. Fits to the XMCD data using atomic multiplet calculations [20], show that the majority of the XMCD is due to octahedral Co (~70%) with a 30% tetrahedral contribution.

Figures 3b & 3c show the Fe XAS and XMCD for $\delta = 0.2$ and $\delta = 0.4$ respectively. The XAS lineshape is similar to that for $\delta = 0$, however, atomic multiplet fits to the XMCD data reveal a smaller tetrahedral / octahedral ratio, (24:76) for $\delta = 0.2$ and (22:78) for $\delta = 0.4$, compared to $\delta = 0$. We note that the amount of Fe^{2+} is the same for all samples to within error.

XAS and XMCD at the Co $L_{2,3}$ edges for $\delta = 0.2$ and 0.4, Fig.3(e,f), show differences in the XAS and XMCD lineshape compared to $\delta = 0$. A comparison of the XAS and XMCD data with an atomic multiplet calculation shows that the magnetic contribution from Co has now significantly changed to a situation where Co^{2+} ions in trigonal sites becomes more important as δ increases (O_h:T_d:C_{3i} = 55:23:22, 59:17:24 for $\delta = 0.2$ and 0.4 respectively). As δ increases, less Co is doped into the S-block so we expect the amount of T_d Co to decrease, as found experimentally. As can be seen from the change in sign of the Co^{2+} XMCD (shown in Fig.3 e, and f) the spins of the tetrahedral / trigonal co-ordinated Co^{2+} align anti-parallel with respect to the the octahedral Fe sites.

4. DISCUSSION

For $\delta = 0.0$ the Co XAS lineshape can be modelled by a superposition of octahedral and tetrahedral Co^{2+} spectra. For $\delta = 0.0$ the Ti-Co substitution is intended to occur only in the S-block i.e. the 2a, $4f_1$ and 12k sites. It has been shown [2,7,21] that Ti has a strong preference for the 12k sites whilst Co^{2+} prefers the $4f_1$ and the 2a sites, although there is significant contradiction in the literature [7,21,22]. The preference for Co^{2+} in the tetrahedral ($4f_1$) sites is reported to be due to the large Co^{2+} cation radius ($r_{Co(2+)}$ = 0.58 Å) which stabilizes the S block compared to the smaller Fe^{3+} cation ($r_{Fe(3+)}$ = 0.49 Å) [21,23]. However, Fe^{2+}, which has a larger ionic radius ($r_{Fe(2+)}$ = 0.63 Å) than Co^{2+}, may modify this picture and force the Co^{2+} into the 2a or 12k sites. The XMCD spectrum clearly shows that the total magnetic contribution from the Co sites is predominantly from Co^{2+} octahedrally co-ordinated.

For $\delta = 0.2$ the Co XAS spectra is a superposition of octahedral, trigonal and tetrahedral Co^{2+} spectra. As doping now takes place in the R and S block we consider that all sites can be occupied. A large change in the coercivity is seen for this sample which is likely to be due to substitution into the trigonal 2b site which is known to be responsible for the large anisotropy in the parent compound [2]. The magnetic contribution from the Co has a component anti-parallel to the Fe octahedral sites and a good fit to the XMCD spectra is based on a ~ 55:23:22 ratio of octahedral: tetrahedral: trigonal. The Co moment on the trigonal site is anti-parallel to the majority of octahedral Fe cations which is in agreement with the finding of Williams *et al* for BaTiCoFeO [22].

For $\delta = 0.4$ the XAS and XMCD at the Co $L_{2,3}$ edges show an intriguing effect. Although the XAS spectra is dominated by Co^{2+} octahedrally co-ordinated, the XMCD shows that the magnetic response is almost identical to that for $\delta = 0.2$. This can be explained by the fact that octahedral Co with opposite spins which contribute additively to the XAS cancel each other out in the XMCD.

The importance of Co^{2+} in the bi-pyramidal trigonal sites to the macroscopic magnetic properties such as the coercivity and magnetoelectric effect is intriguing. Recently the role of the bi-pyramidal trigonal to ME effects in hexaferrites has been studied by Shen *et al* [12] in which the authors show that the competition between long range Coulomb interactions and short range Pauli repulsion in a $(TM)O_5$ bipyramidal unit favours an off centre displacement of the TM ion inducing a local electric dipole. To provide further insight we simulated the M-type hexaferrite structure using Materials Studio [24]. Two

structures were created to replicate (a) strontium hexaferrite, $SrFe_{12}O_{19}$, in which Fe^{3+} ions occupy all interstitial lattice sites, and (b) a strontium hexaferrite with Co^{2+} ions substituted at the trigonal bi-pyramidal sites and Ti^{4+} substituted into the 12k sites. The geometries were optimised using the CASTEP 8.0 density functional theory (DFT) code [25] with calculations performed using the General Gradient Approximation (GGA) and the Perdew-Burke-Ernzerhof (PBE) functional. Having performed geometry optimisation calculations the in plane and out of plane trigonal bi-pyramidal site bond lengths, r_0 and r_1, were extracted.

Using the phenomenological local potential energy method for the bipyramid, as developed in [12], the energy profile along the c-axis (z) was calculated using

$$U_{repulsion}(z) = 3\beta c_{+-} exp\left[\left(r_+ + r_- - \sqrt{r_0^2 + z^2}\right)/\rho\right] + \beta c_{+-} exp[(r_+ + r_- - (r_1 + z))/\rho] + \beta c_{+-} exp[(r_+ + r_- - (r_1 - z))/\rho]$$

Eq. (2)

where r_0 and r_1 are the in-plane and out-of-plane TM-O distances in the bi-pyramid for 2b sites, β is a constant (taken to be 1.35×10^{-19} J), $c_{+-} = 1$ is Pauling's valence factor, and $\rho = 0.314$ Å [26]. $r_+ = 0.58$ (0.67) Å are the ionic radii of Fe^{3+} and Co^{2+} with a co-ordination number of 5 respectively and $r_- = 1.4$ Å is the ionic radius of O^{2-} from [23].

The local potential energy profile along the c-axis for SrM where Fe^{3+} resides in the 2b site is shown in Fig.4a. The energy barrier (ΔE) for SrM is only 2meV so that at room temperature an "average" equatorial position is expected providing no polarization. However on substitution of Co^{2+} and Ti^{4+} into the 2b and 12k positions respectively the situation changes [27,28], Fig.4b. The separation of the minima increases from 0.3 Å to 0.8 Å whilst the energy barrier increases from 2 to 120 meV. Wang *et al* [29] have also investigated the structural instability of the trigonal bi-pyramidal site for the M-type hexaferrite and demonstrate that that the ferroelectric state is energetically favourable in an external electric field. Although in Co-Ti doped hexaferrites not all the cations in the 2b sites will be substituted by Co, an increase in Co into these sites, as evidenced by the XAS/XMCD data, enhances the ability for the structure to polarize as well as providing a magnetoelastic ion. As such, local distortions introduced by the Co ions in the 2b sites affect the piezoelectric strain coefficient as well as the magnetoelastic coupling. The combination of the two provides a route to increase the magnetoelectric coupling coefficient as was first shown theoretically in [10] where an additional term can be added to α which is proportional to the product of the magnetoelastic and piezoelectric tensors of the material. Further evidence of this is provided by the reduction of Λ_2 above 300V which is indicative of piezoelectric strain - voltage characteristics. Therefore, it seems that Co substitution into the 2b trigonal sites provides a mechanism for enhancing the magnetoelectric effect in this material.

5. SUMMARY AND CONCLUSIONS

In summary, we have used a combination of VSM magnetometry XAS / XMCD at the Fe and Co $L_{2,3}$ edges to study the effect of Co substitution on the magnetoelectric coefficient in Co-Ti doped SrM hexaferrites. Multiplet features in the Co XMCD in combination with ME measurements suggest that Co entering the trigonal 2b sites play an important role in the magnetoelectric effect in these materials.

Supplementary Material

The unit cell of $SrFe_8Ti_2Co_2O_{19}$. The key indicates Wyckoff positions, point group symmetry and block of the various cation sites.

Acknowledgements

The authors would like to acknowledge Professor M. J. Probert for fruitful discussions and to Diamond Light Source for the provision of beamtime under SI-10361, SI-12565 and SI-14135.

References

[1] Y. Kitagawa, Y. Hiraoka, T. Honda, T. Ishikura, H. Nakamura and T. Kimura. Nature Materials **9**,797 (2010)

[2] R.C. Pullar. Progress in Materials Science **57**, 1191 (2012)

[3] J. Smit and H. P. J. Wijn. Ferrites. Philips Technical Library, (1959)

[4] A Tauber, J. A. Koctahedraln and R. O. Savage. J Appl Phys 34, 1265 (1963)

[5] M. Soda, T. Ishikura, H. Nakamura, Y. Wakabayashi and T. Kimura. Phys. Rev. Lett. **106**, 087201 (2011)

[6] P. Borisov, J. Alaria, T. Yang, S. R. C. McMitchell and M. J. Rosseinsky. Appl. Phys. Lett. **102**, 032902 (2013)

[7] L. Wang, D. Wang, Q. Cao, Y. Zheng, H. Xaun, J. Gao and Y. Du. Sci. Rep **2**, 223 (2012)

[8] M. Mohebbi, K. Ebnabbasi, and C. Vittoria. J. Appl. Phys. **113**, 17C710 (2013)

[9] G. F. Dionne, "Magnetic Oxides", Springer (2009)

[10] C. Vittoria, S. Somu and A. Widom, Phys. Rev. B **89**, 134413(2014)

[11] C. Jia , S. Onoda, N. Nagaosa and J. H. Han. Phys. Rev. B **74**, 24444 (2006)

[12] S-P. Shen, Y-S. Chai, J-Z. Cong, P-J. Sun, J. Lu, L-Q. Yan, S-G. Wang and Y. Sun. Phys. Rev. B **90**, 180404(R) (2014)

[13] R. Karim and C. Vittoria, JMMM 167, 27(1997); A. Geiler, A. Yang, X. Zuo, S. Dae Yoon, Y.Chen, V. G. Harris, and C. Vittoria.. Phys. Rev. Lett. 101, 067201 (2008)

[14] S. S. Dhesi, S. A. Cavill, A. Potenza, H. Marchetto, R. A. Mott, P. Steadman, A. Peach, E. L. Shepherd, X. Ren, U. H. Wagner, *et al. AIP Conference Proceedings* **1234**, 311 (2010)

[15] W. Eerenstein, N. D. Mathur and J. F. Scott. Nature **442**, 759 (2006)

[16] M. Javed Iqbal, M. Ashiq and I. H. Gul. Journal of Magnetism and Magnetic Materials **322**, 1720 (2010)

[17] H. Izadkhah, S. Zare, S. Soma and C. Vittoria. Appl. Phys. Lett. **106**, 142905 (2015)

[18] Core level spectra were simulated using the CTM4XAS software (E. Stavitski and F.M.F. de Groot, Micron **41**, 687 (2010)) with the following parameters: 10Dq (Octahedral) = 1.9eV, 10Dq (Tetrahedral) = -0.9eV with Slater parameters reduced to 80% of the HF values. The Lorentzian broadening values used for each peak in the simulated spectrum were 0.1 eV, 0.6 eV, 0.5 eV, and 1.0 eV respectively. G. van der Laan and B.T. Thole, Phys. Rev. B **43**, 13401 (1991).

[19] D.J. Huang, C. F. Chang, H-T. Jeng, G. Y. Guo, H-J, Lin, W. B. Wu, H. C. Ku, A, Fujimori, Y. Takahashi and C. T. Chen. Phys. Rev. Lett **93**, 077204 (2004)

[20] The following parameters were used for the calculations. 10Dq (Octahedral) = 1.1eV, 10Dq (Tetrahedral) = -0.5eV with Slater parameters reduced to 72% of the HF values. For the trigonal bipyramidal sites the C3i symmetry was used with 10Dq = 0.8eV, Dτ = -0.08eV and Dσ = 0.01eV. We note for these values of the crystal field parameters the five d-orbitals break up into two doublets ^{2}E''(d_{zx}, d_{yz}) and ^{2}E'($d_{x^2-y^2}$, d_{xy}) plus a singlet $^2A_1'$ (d_{z^2}) with $^2A_1'$ > ^{2}E' > ^{2}E'' as expected for this symmetry.

[21] J. Kreisel, H. Vincent, F. Tasset, M. Pate and J. P. Ganne. J. Magn. Magn. Mater. **224**, 17 (2001). X. Batlle, X. Obradors, J. Rodriguez-Carvajal, M. Pernet, M. V. Cabanas and M. Vallet. J. Appl. Phys. **70**, 1614 (1991).

[22] J. M. Williams J. Adetunji and M. Gregori. JMMM **220**, 124 (2000)

[23] R.D. Shannon, Acta Crystallogr. A 32 (1976) 751.
[24] Accelrys Inc. *Materials Studio*, version 8.0; Accelrys Inc.: San Diego, CA, USA, 2016
[25] S. J. Clark, M. D. Segall, C. J. Pickard, P. J. Hasnip, M. J. Probert, K. Refson and M. C. Payne. Zeitschrift fuer Kristallographie 220, 567 (2005)
[26] S. P. Marshall and J. B. Sokoloff. Phys. Rev. B **44**, 619 (1991)
[27] A.S. Mikheykin, E.S. Zhukova, V.I. Torgashev, A.G. Razumnaya, Y.I. Yuzyuk, B.P. Gorshunov, A.S. Prokhorov, A.E. Sashin, A.A. Bush and M. Dressel. Eur. Phys. J. B 87,232 (2014)
[28] For Co^{2+} in the bi-pyramidal trigonal sites r_0, r_1 and r_+ are 1.9065 Å, 2.3872 Å and 0.67 Å respectively.
[29] P. S. Wang and H. J. Xiang. Phys. Rev. X **4**, 011035 (2014)

Figure Captions

Figure 1: Change in |M| as a function of applied voltage, V, for $\delta = 0.0$, $\delta = 0.2$ and $\delta = 0.4$. Measurements were taken at T= 300K with an applied bias field of 400 Oe with E parallel to M. Inset: M – H curves for $\delta = 0.0$, $\delta = 0.2$ and $\delta = 0.4$ at T = 300K.

Figure 2: Ti $L_{2,3}$ XAS measured for $\delta = 0.2$ at 300K in TEY (red data points). The blue solid line is the simulated spectra from an atomic XAS multiplet calculation of Ti^{4+} in an octahedral co-ordination with 10Dq = 1.9 eV.

Figure 3: Experimental XAS (red) and XMCD (green) spectra for (a) $\delta = 0.0$, (b) $\delta = 0.2$ and (c) $\delta = 0.4$ at the Fe $L_{2,3}$ edges. Atomic multiplet simulations of the XMCD are shown in black on topof the experimental XMCD. Experimental XAS (red) and XMCD (green) spectra for (d) $\delta = 0.0$, (e) $\delta = 0.2$ and (f) $\delta = 0.4$ at the Co $L_{2,3}$ edges. Fits to the XMCD data using atomic multiplet calculations are shown in black. Spectra were measured at T = 230K, $\mu_0 H = 6T$ and with the X-ray propagation vector parallel to H and at 60 degrees with respect to the surface normal.

Figure 4: The calculated energy potentials from Eq. (2) for $U_{repulsion}$ as a function of off-equatorial displacements (z) for (a) Fe^{3+} and (b) Co^{2+} in the trigonal bi-pyramidal site and Ti^{4+} in the octahedral 12k site.

Figure 1

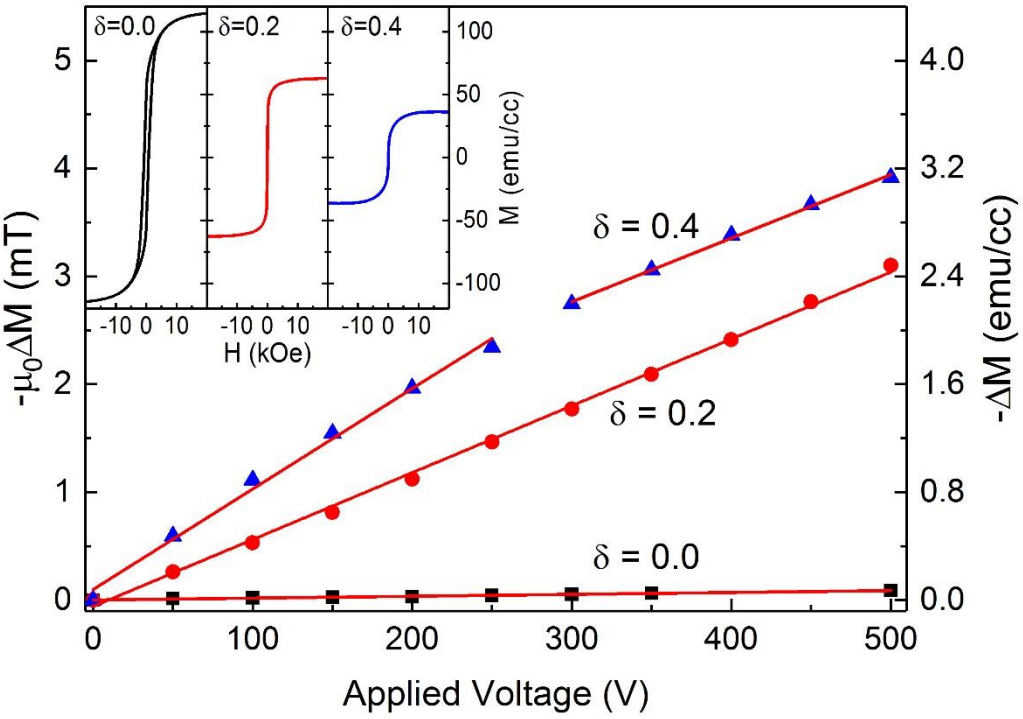
δ=0.0
δ=0.2
δ=0.4
-10 0 10
H (kOe)
100
50
0
-50
-100
M (emu/cc)
δ = 0.4
δ = 0.2
δ = 0.0
-μ0ΔM (mT)
-ΔM (emu/cc)
Applied Voltage (V)
0
100
200
300
400
500
0
1
2
3
4
5
0.0
0.8
1.6
2.4
3.2
4.0

Figure 2

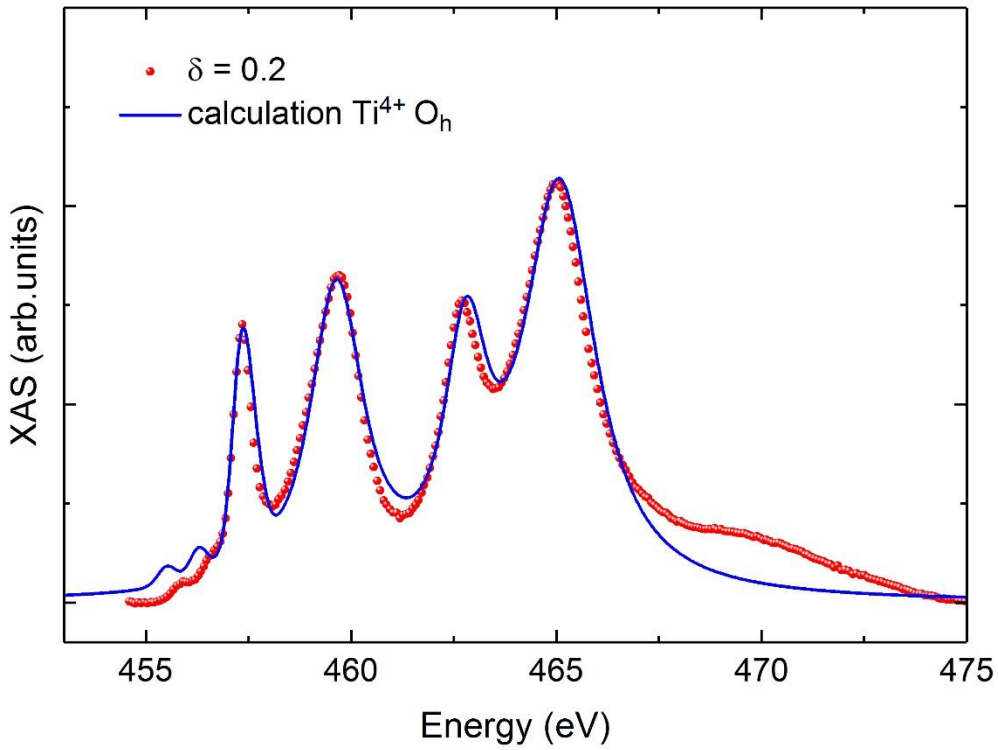
δ = 0.2
calculation Ti4+ Oh
XAS (arb.units)
455
460
465
470
475
Energy (eV)

Figure 3

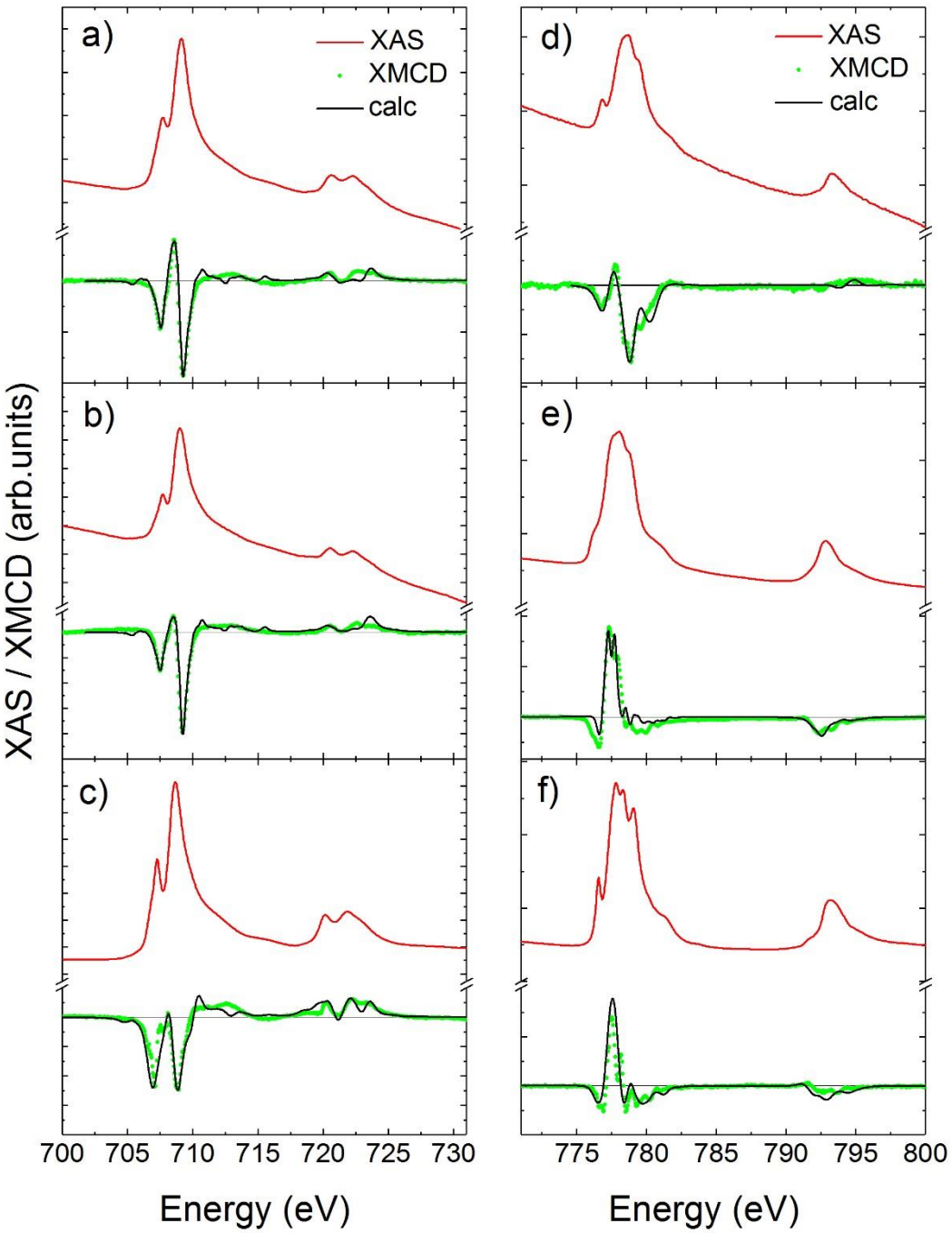
a)
b)
c)
d)
e)
f)
XAS
XMCD
calc
XAS / XMCD (arb.units)
700 705 710 715 720 725 730
775 780 785 790 795 800
Energy (eV)
Energy (eV)

Figure 4

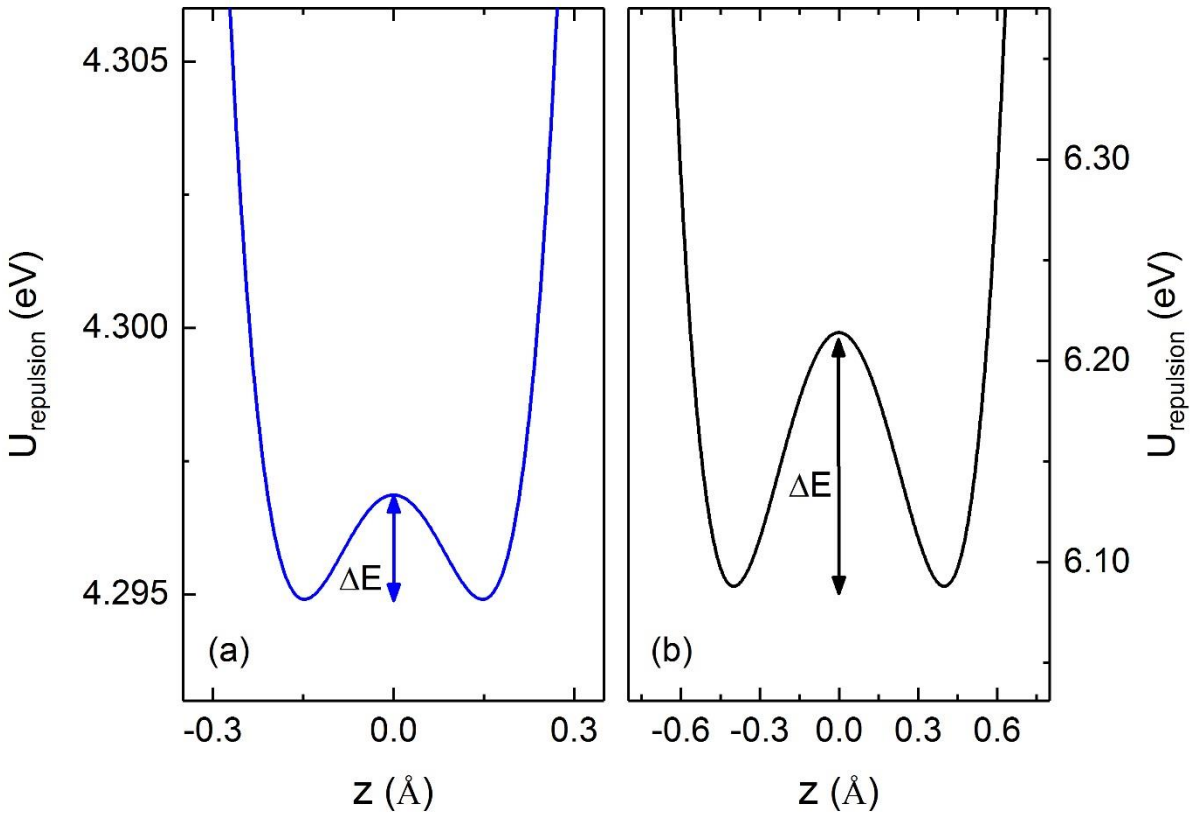
4.305
4.300
4.295
$U_{repulsion}$ (eV)
ΔE
(a)
-0.3
0.0
0.3
z (Å)
6.30
6.20
6.10
$U_{repulsion}$ (eV)
ΔE
(b)
-0.6
-0.3
0.0
0.3
0.6
z (Å)